NASA CONTRACTOR REPORT

NASA CR-93

NASA CR-93

CELLULAR ALUMINUM FOR USE IN ENERGY DISSIPATION SYSTEMS

by S. Lipson

Prepared under NASA Purchase Request L-18, 381 *by*
FRANKFORD ARSENAL
United States Army
Philadelphia, Pa.
for

NATIONAL AERONAUTICS AND SPACE ADMINISTRATION • WASHINGTON, D. C. • SEPTEMBER 1964

CELLULAR ALUMINUM FOR USE IN

ENERGY DISSIPATION SYSTEMS

By S. Lipson

Prepared under NASA Purchase Request L-18, 381 by
FRANKFORD ARSENAL
United States Army
Philadelphia, Pennsylvania

for

NATIONAL AERONAUTICS AND SPACE ADMINISTRATION

For sale by the Office of Technical Services, Department of Commerce,
Washington, D.C. 20230 -- Price $1.00

TABLE OF CONTENTS

T: FRA

INTRODUCTION

This study was initiated under the sponsorship of the NASA Langley Research Center for the purpose of developing cellular aluminum structures for use in energy dissipation systems. These cellular structures are attractive for such applications because of their inherent isotropic properties and their great capacity for energy absorption through collapse of the cells in the structure. Since the specific applications are intended for space exploration, the problem of energy absorption capacity per unit of weight is also of the greatest importance. These materials will be required to absorb energy at loading rates which will not exceed 100 feet per second. Prior work at NASA Langley Research Center has shown that the results obtained with slow speed compression tests correlate with the results obtained at the anticipated rates of loading. In order to expedite the study, testing for material evaluation was confined to the slower speeds obtainable with conventional testing machines.

The cellular aluminum materials under consideration are particularly adaptable for fulfillment of these requirements. The size, shape, and size distribution of the open cells in the structure can be controlled with precision, and the scope for alloy selection covers the entire range of aluminum alloy materials. The basic material was developed during an earlier study,* and it is manufactured by the infiltration of a porous briquette of a soluble substance with molten metal. The soluble briquette used for light alloys is formed by sintering a suitably graded aggregate of rock salt (NaCl). After solidification of the molten metal, the soluble component is removed by leaching and the cellular metal structure remains. This study was directed toward identification and measurement of the important parameters which control the apparent density, compressibility, material quality, and energy absorption characteristics of the cellular aluminum.

METHODS AND MATERIALS

Preparation of Material

The test material for this study was prepared in the form of 2.25 in. diameter cylinders, approximately 5 in. long. Figure 1 is a schematic

*L. Polonsky and S. Lipson, "A New Type of Lightweight Cellular Material," Frankford Arsenal Report R-1534, April 1960.

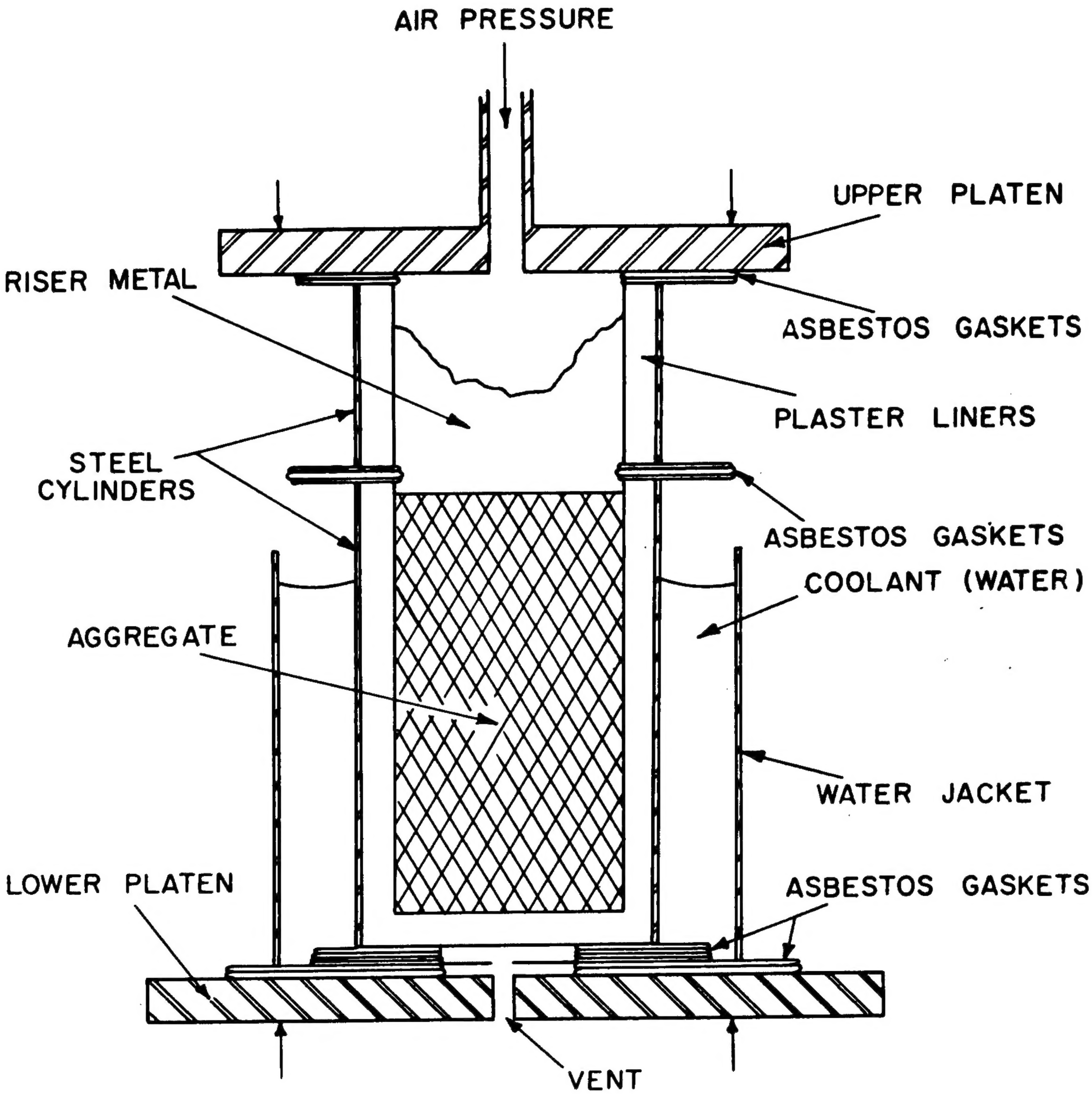

Figure 1. Schematic illustration of Method for Infiltration of Soluble Aggregate and Solidification of Cellular Metal Castings

illustration of the apparatus used for casting and solidification of the cellular material. The following procedure was employed.

Mold Preparation

Two 3-in. diameter steel tubes are lined with a 1/4 in. thickness of plaster. The upper cylinder is short and serves as a hot top, or riser; the lower and longer cylinder acts as the mold. The plaster lined cylinders are calcined at 500° F for 2 to 4 hours. After cooling to room temperature, the mold is filled and maximum compaction of the salt particles is achieved by vibration. The filled mold is returned to the furnace and heated for 12 to 18 hours at 1350 to 1400° F. The temperature is then lowered to 1250° F before casting. The riser sleeve is similarly heated to 1250° F prior to casting.

The elevated temperature treatment serves to sinter the particles of salt aggregate. The high temperature baking also causes shrinkage of the aggregate and, as a consequence, the apparent density of the final cellular metal product is reduced because the proportion of voids in the soluble briquette governs the percentage of metal in the cellular casting. In addition, this treatment increases the dimensions of the intercellular channels, and this tends to facilitate leaching of the soluble aggregate from the final casting.

Cell Structure Control

One of the important characteristics of the material produced by this process is the precise control of the cellular structure. While some of the other process parameters affect the geometry of the cellular structure, the principal area of control lies in the size and shape distribution of the aggregate used to fill the mold. In order to simplify the exploratory phases of this investigation, a standard distribution aggregate was adopted. This aggregate corresponded to the commercial table salt grade, which is composed of cubic crystals. The sieve analysis of this grade is given in Table I. Changes in cell structure were achieved either by removing certain sieve fractions from the standard distribution aggregate or by blending appropriate sieve fractions of crushed salt particles. The latter material differed from the standard with respect to particle shape. The crushed particles should be classified as angular, rather than cubic.

TABLE I. Sieve Analysis of Standard Distribution Salt Aggregate

(Grade: Table Salt; Particle shape: cubic)

Mesh	U.S. Std Sieve No.	Sieve Opening Microns	Sieve Opening Inches	Weight (%)
20	20	883	0.0331	Trace
28	30	589	0.0234	0.49
35	40	414	0.0166	18.85
48	50	295	0.0117	55.38
60	60	250	0.0098	16.62
100	100	147	0.0059	7.77
Pan	Pan	-	-	0.89

The following cellular structures, classified by the type of salt aggregate used in their manufacture, were evaluated in the course of this investigation:

(1) Standard sieve distribution.

(2) Duplex distribution (coarse particles with the interstices filled by fine particles).

(3) Other sieve distributions. A few tests were conducted with an insoluble aggregate contained in the structure. This was a proprietary material marketed under the name Kanamite. It consists of hollow ceramic spheres having a bulk density of 0.3 to 0.4 g/cc. Since this aggregate is not removed, as is the case with the salt, the apparent density of the composite structure is increased by the contribution of the aggregate retained in its structure.

Casting Procedure

The mold and riser are removed from the furnace and positioned between platens, as shown in Figure 1. The riser sleeve is filled with molten metal and the platens are closed. The asbestos gaskets prevent leakage of metal between the mold and riser, and prevent the coolant from coming in contact with the plaster surface at the bottom of the mold during the period of solidification.

The air pressure is then slowly raised to 50 psi. With fine mesh aggregates, the metal will not infiltrate until pressure is applied. After one minute, water is admitted into the coolant jacket. This develops the thermal gradient necessary for progressive solidification. Pressure is maintained until solidification is complete - approximately eight minutes for the mold geometry shown in Figure 1. The water is then drained, the platens separated, and the mold removed and allowed to cool before further processing.

Heat Treatment

It was anticipated that the interconnecting structure of the cellular material would promote response to heat treatment. However, this did not prove to be the case because the fine structures employed in these studies did not permit the free flow of quenching water through the structure. Steam was generated within the structure and prevented the quenching water from entering the cells. As a result, it was found that heat treatable alloys did not show the expected response to standard precipitation hardening treatment.

An attempt was made to quench the structure by clamping the specimen between two platens and forcing water into both ends of the material. This was found to improve response to heat treatment, but the problem of steam formation within the fine structure was not completely resolved. The most satisfactory method found was to heat-treat prior to leaching. Even though the thermal conductivity of the salt phase is low, it is still much greater than that of the steam formed in the structure when open cell quenching methods are employed.

Another advantage of deferring the leaching operation until after solution heat treatment is that the presence of the salt phase tends to prevent oxide formation on the cell wall surfaces. Since solution treatment is usually performed in air furnaces at temperatures up to 1000° F for long periods of time, substantial oxide thicknesses would otherwise be formed over the large exposed surfaces in the cellular structure. Table II gives the heat treatment schedules used for the various materials tested.

Machining

Like other types of open cell materials, cast cellular alloys present some difficulties in machining. The usual solution to these problems is to provide some temporary support for the cell walls, to prevent

TABLE II. Heat Treatment Schedule for Aluminum Alloys

Alloy	Solution Treatment Temp (°F)	Solution Treatment Time (hr)	Aging Treatment Temp (°F)	Aging Treatment Time (hr)
356-T6	1000	18*	310	5
195-T6	960	18*	310	5
220-T4	830	20*	-	-
7075-T6	860	64	-	-
2-step Solution Treated	880	24[a]	250	24
2024-T6	900	16[a]	375	12
122-T6	950	12[a]	340	8

[a]Cold water quench after time at temperature.

smearing of the structure. These materials, however, have a "built-in" support by virtue of the soluble salt phase. Accordingly, if machining is performed prior to leaching, close machining tolerances and excellent surface finishes can be obtained.

It was found that slow speeds tend to prolong cutting tool life. Heavy cuts and coarse feeds also favor the machinability of the alloy. High machining speeds and fine cuts tend to cause the cutting edge of the tool to become heated and fail through abrasion by the salt phase in the structure.

Leaching

The brines generated during the leaching process tend to be corrosive to the metal. The rate at which the salt can be leached, therefore, becomes a matter of importance if corrosion during this phase of the process is to be minimized. In addition, more efficient leaching permits use of finer cell material. Accordingly, a limited study of leaching rates was made in the course of specimen preparation. Figure 2 shows the effect of thermal treatment of the salt briquette on the leaching rate. Leaching rate increases with time at temperature because the intercellular channels become larger as the particles in the aggregate tend to fuse together.

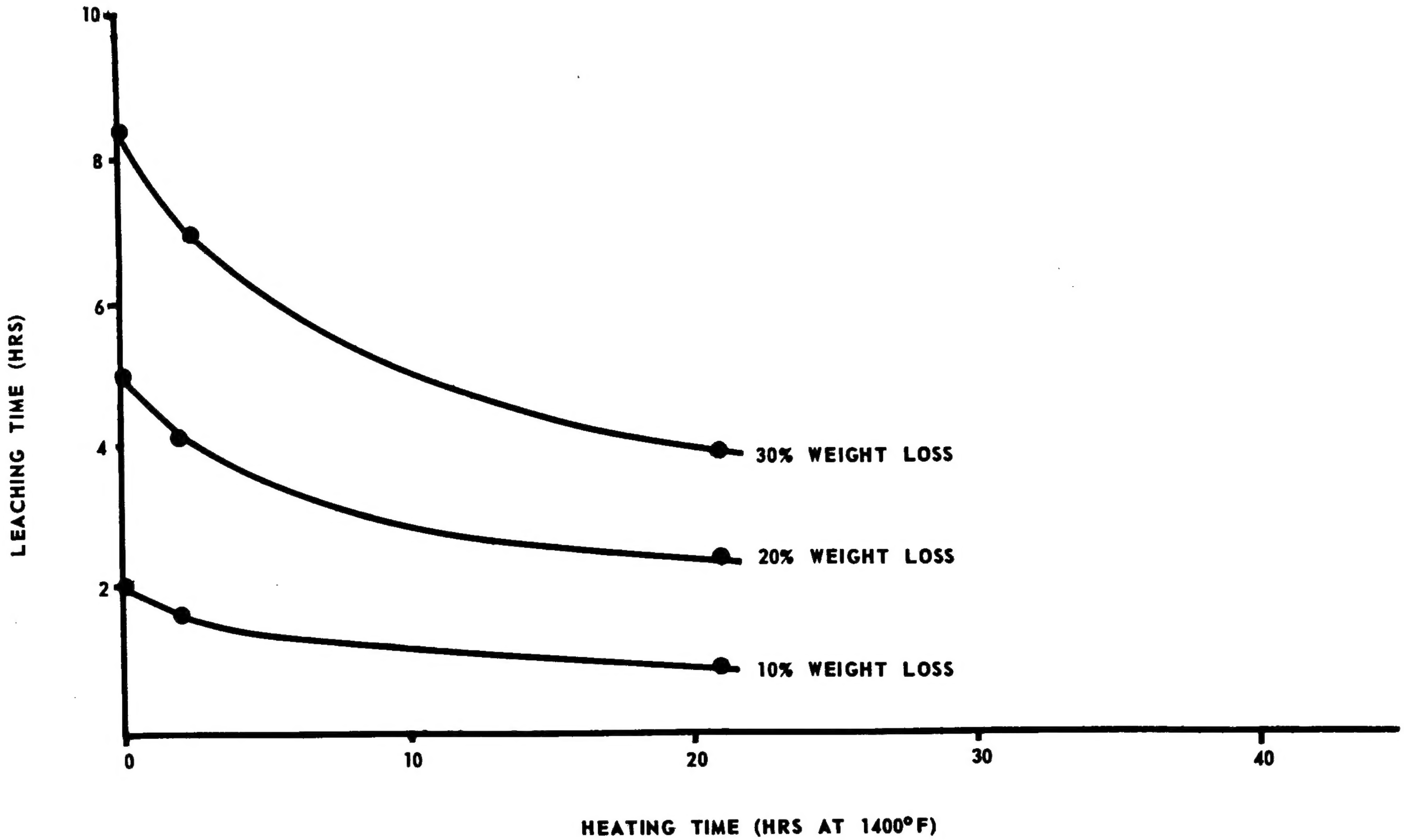

Bath size: 1 gallon; Specimen size: 2 in. dia by 2 in. long; Water change: 1 hr intervals

Figure 2. Effect of Thermal Treatment on Leaching Rate (Static)

In order to accelerate salt removal significantly, it is necessary to employ some kind of forced leaching practice. Prior work has shown that agitation of the leaching bath has no effect on the leaching rate because the cellular structure inhibits effective agitation of the leaching liquor in contact with the salt in the interior of the material.

Further consideration of the leaching process indicated the principal mechanism for removal of the salt is gravity convection. The denser salt-laden liquor in contact with the salt crystals flows down through the structure to the bottom of the container, and less dense liquor moves in to take its place. One possible means for speeding this process is to promote the gravity separation by centrifuging the bath. Figure 3 shows the effect of centrifuging the leaching bath and specimen on the leaching rate. In this test, the bath volume was small and the specimen was placed at the center of rotation. Subsequent tests with a larger bath and the specimen placement midway between the axis of rotation and the walls of the container showed far greater rates of salt removal.

Density Control

The process for manufacture of cellular metals does not readily permit control of apparent density beyond certain fairly narrow limits. A limited exploratory study of means for broadening the range of material density was made. The following methods were examined:

(1) Sintering - The salt briquette is heated at temperatures close to the melting point of the salt.

(2) Duplex Structures - A coarse basic cell structure with a fine cellular interstitial structure is used to reduce the amount of material in the webs.

(3) Cell Size Distribution - A standard distribution aggregate is being used during the early phase of this investigation. However, optimum ranges of cell size distribution are being sought.

(4) Metal Duplication of Organic Packaging Materials - An investment-like material made from the salt is used to invest the fibers of organic packaging-type materials. The fibers are eliminated by oxidation at high temperature burnout and the metal is introduced to duplicate the organic structure in metal. The salt investment is easily removed by leaching.

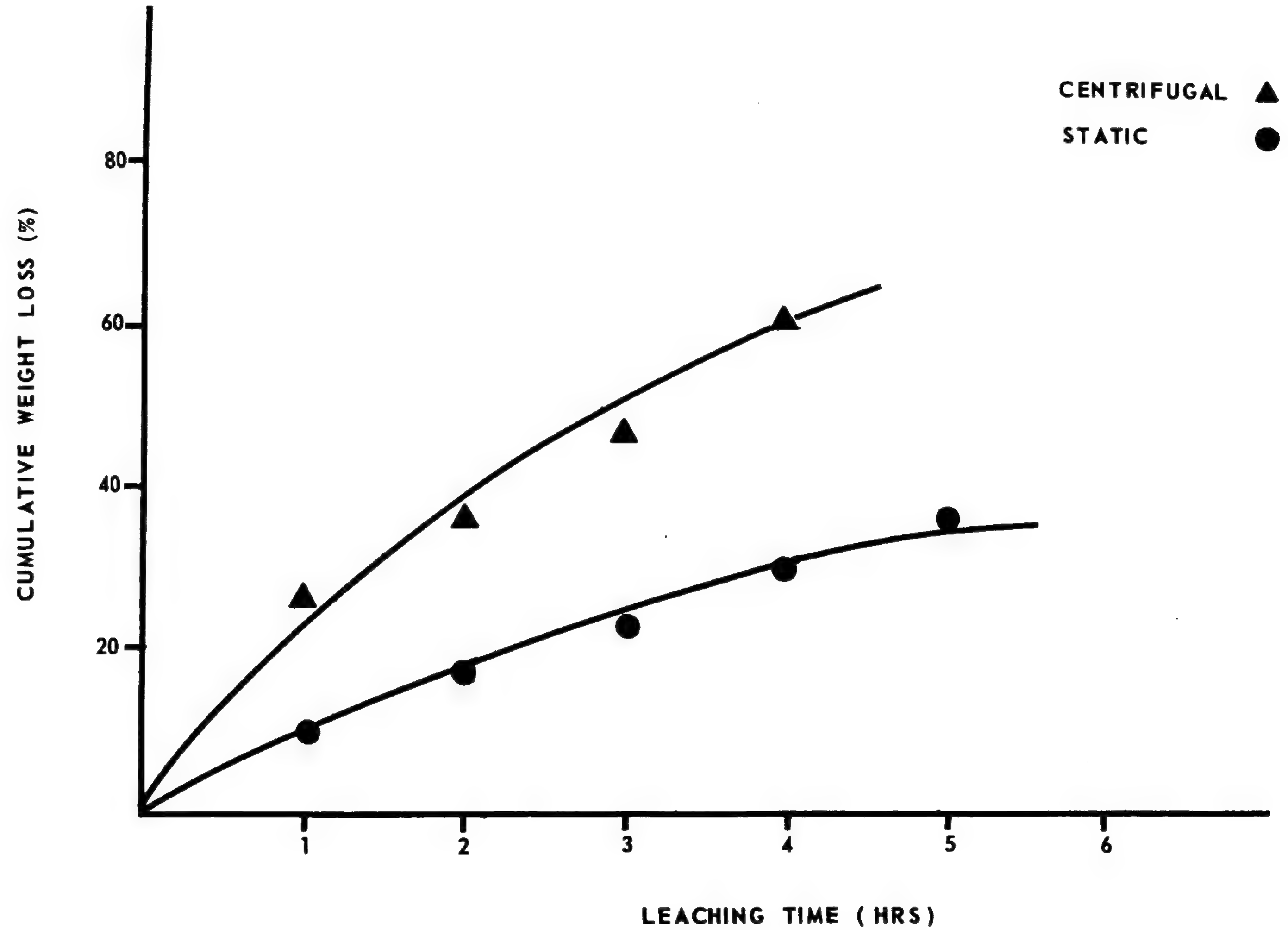

Bath size: 1 gallon; Specimen size: 2 in. dia by 2 in. long; Water change: 1 hr intervals

Figure 3. Effect of Centrifuge on Leaching Rate

The following conclusions were drawn as a result of this investigation:

(1) Sintering - Prolonged heating of the salt briquette was found to be moderately effective in reducing the void volume of the briquette. This reduced the weight of metal that could be infiltrated, hence the lowered density of the cellular sample. After 46 hours at 1400° F, the apparent density of a cellular aluminum alloy was reduced from approximately 0.88 g/cc to 0.82 g/cc. Although the melting point of sodium chloride is 1474° F, difficulties were experienced in control of the sintering operation at temperatures above 1400° F.

(2) Duplex Structures - Duplex structures were obtained by first sintering coarse salt aggregate (6, 8, and 10 mesh) at 1400° F for 2 hours, cooling to room temperature, and infiltrating the resultant briquette with a fine aggregate (60 mesh). The apparent density of these structures was approximately half of the values obtained with the standard distribution aggregate. The lowest density was obtained with the 6 mesh/60 mesh combination (0.355 g/cc).

(3) Cell Size Distribution - The standard sieve distribution was found to result in an approximately 10 percent reduction in apparent density over the cellular structures produced with a single sieve fraction. This was true over the range examined, 30 mesh through 60 mesh. The effect on apparent density produced by varying the relative proportions of a two-sieve fraction aggregate was also determined. This differed from the duplex structures in that the fine and coarse fractions were thoroughly mixed before filling the mold cavity. The optimum ratio of cell diameters was first determined by mixing coarse and fine sieve fractions over a range of proportions and the maximum density aggregate determined. Figure 4 shows these data and indicates that a 40-60 ratio of fine to coarse is optimum. The optimum ratio of particle diameters was determined by mixing various fine sieve fractions with coarse aggregate. It was found that a density plateau was reached when the ratio of particle diameters exceeds 3 (Figure 5). A series of castings was then prepared using 60 percent 12 mesh aggregate as the coarse fraction and 40 percent 48 mesh as the fine. The particle diameter ratio for this mixture was approximately 4.5.

(4) Metal Duplication of Organic Packaging Materials - A limited amount of effort was directed toward developing a technique of fabricating

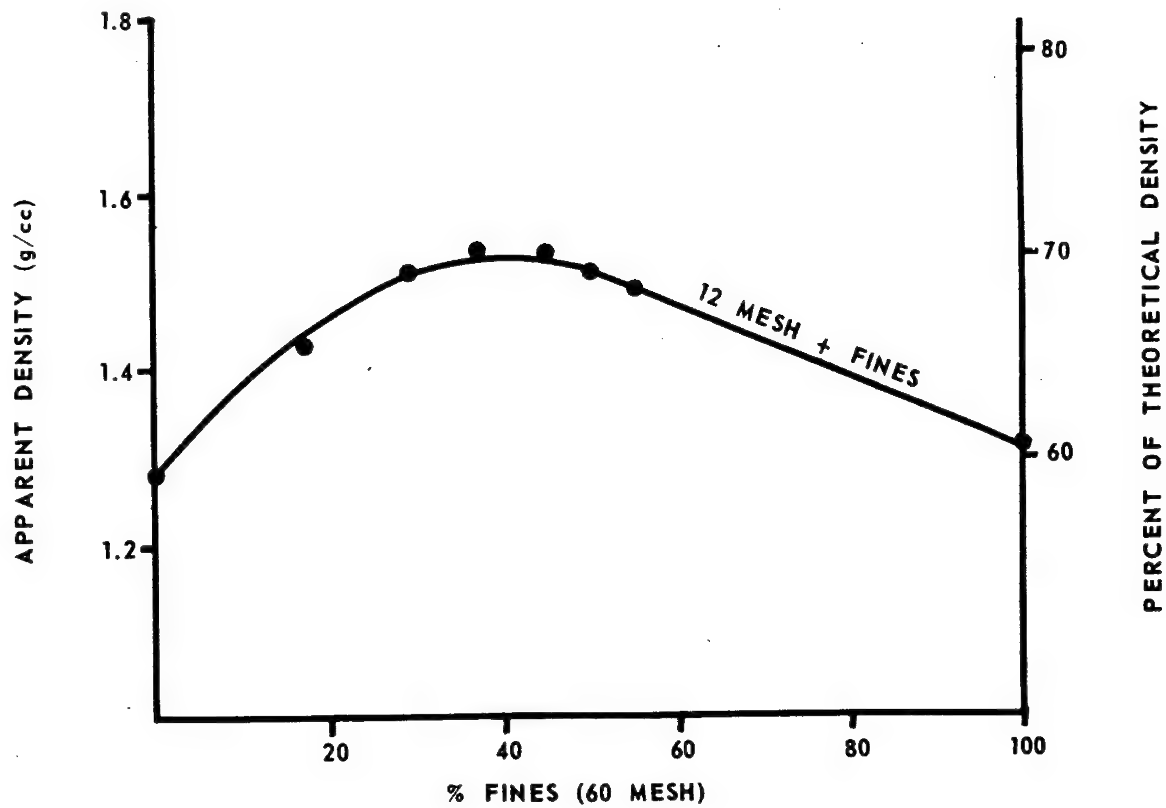

Figure 4. Effect of Percentage Fines on the Apparent Density of a Two-sieve Distribution Salt Aggregate

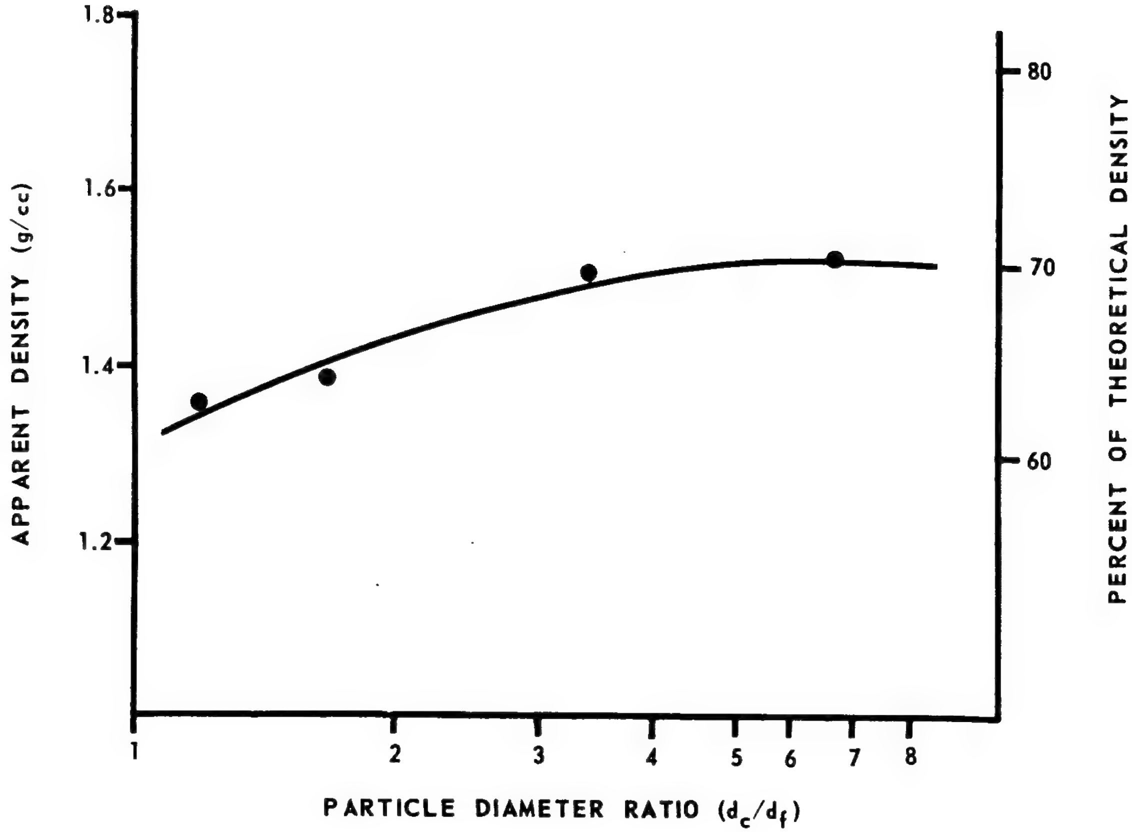

Figure 5. Effect of Particle Diameter Ratio on the Apparent Density of a Two-sieve Distribution Salt Aggregate 40% Fines (Mixture)

fibrous metals. Figure 6 is a sample of metal duplication of excelsior material. It is apparent that the process is feasible; however, much more effort would be required to develop a practical processing technique. It was decided to defer further work along this line in order to concentrate upon the primary objectives of the investigation.

Alloy Selection

In the course of this study a broad range of cellular aluminum alloys was prepared. The compressive behavior of the more significant materials studied will be discussed in the section of the report dealing with compression testing. The nominal composition of the alloys studied are given in Table III.

TABLE III. Nominal Composition and Typical Tensile Properties of Aluminum Alloys

Alloy Designation	Nominal Composition (%)	Strength (psi) Yield	Strength (psi) Tensile	Elongation (% in 2 in.)
356-T6	7 Si-0.3 Mg			
214	3.8 Mg-1.8 Zn	16,000	27,000	7
Almag 35	7 Mg	19,000	35,000	9
220-T4	10 Mg	26,000	46,000	14
195-T6	4.5 Cu	24,000	36,000	5
43	5 Si	9,000	19,000	6
2024-T4[a]	4.5 Cu-1.5 Mg	46,000	68,000	19
7075-T6[a]	5.5 Zn-2.5 Mg	72,000	82,000	10
122-T6	10 Cu	30,000	40,000	<0.5

[a]Wrought material

Specimen Geometry

The basic specimen geometry employed for these tests was a simple cylinder. The length-to-diameter (l/d) ratios were varied in order to explore the effect of this parameter on the compressive behavior

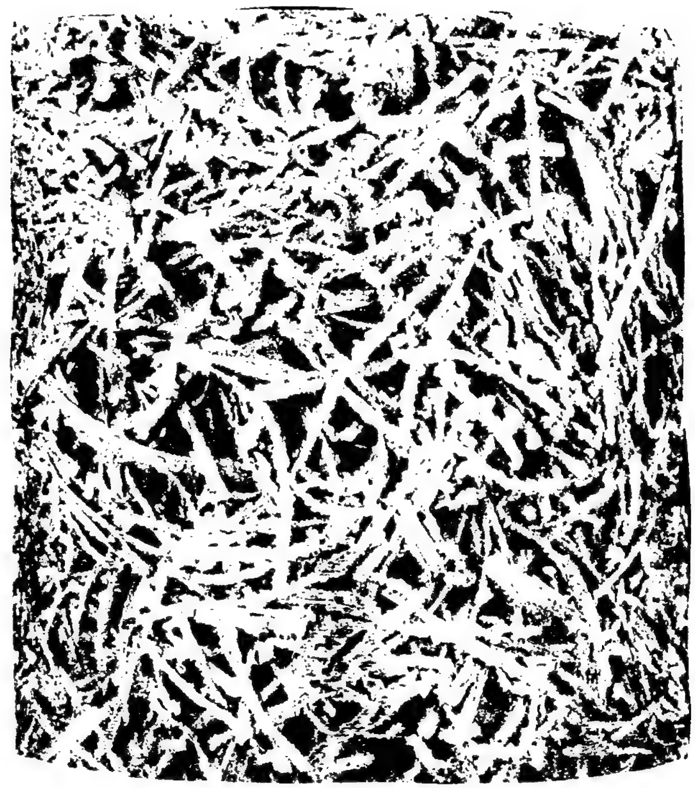

Material: Excelsior/214 Alloy
Mag: 2X

Figure 6. Metal Duplication of Organic Packaging Material

of the material. A limited number of tests was conducted with truncated conical specimens and some tests with composite cylinders. The latter specimens were solid cellular cylinders of one composition, which were pressed into hollow cellular cylinders of another alloy. This was done in the belief that material selection could be made on the basis of complementary properties (i.e., strong hard materials contained in ductile cylinders). These latter tests all gave negative results, and further work on the conical shapes and composite cylinders was abandoned.

Test Methods

The preliminary tests were conducted with a 60,000 lb Tinius Olsen testing machine. The capacity of this machine limited the amount of compression to approximately 50 percent of the specimen length. Later tests were shifted to a larger capacity machine (300,000 lb) and an autographic record of the load deformation characteristics of the material was made. The applied load was limited to 150,000 lb. The rate of loading ranged between 0.3 to 0.5 inch per minute.

RESULTS AND DISCUSSION

Basic Considerations

The goal for this materials development program can be qualitatively defined in terms of an ideal stress deformation curve. Figure 7a is a schematic illustration of the desired load deformation relationship and shows a condition where deformation proceeds at constant load. In an energy dissipation system, this deformation pattern is a prerequisite if deceleration rates are to be kept at a constant level. If the load absorption capacity is sustained through substantially complete destruction of the material, use is made of the full energy dissipation potential inherent in a given material. Of course, the higher the level of constant load, the higher its energy dissipation capacity becomes.

In most cellular metals systems the load deformation pattern tends to be greatly different from that represented as an idealized system, as

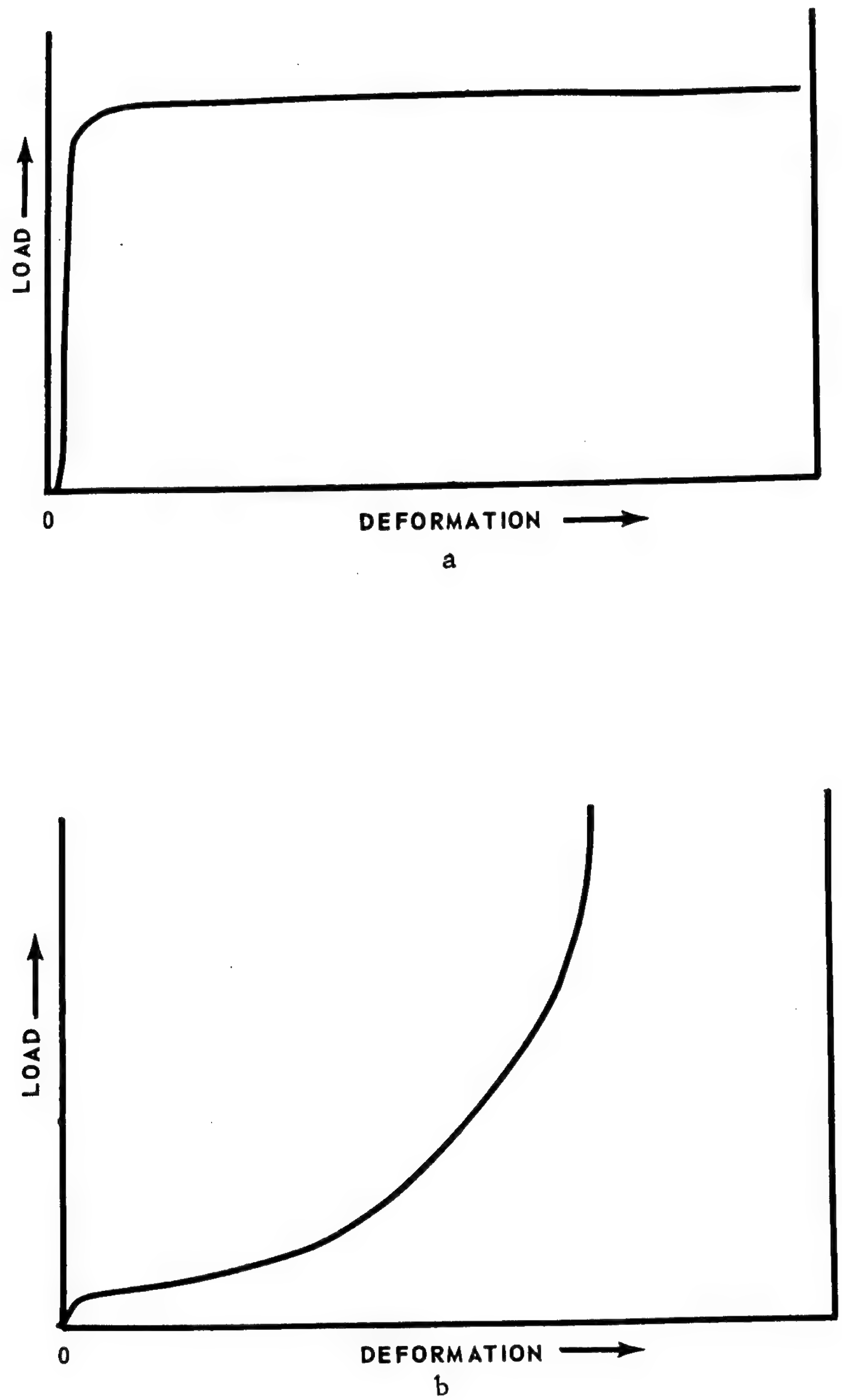

Figure 7. Load-Deformation Relationships in Energy Dissipation Systems

shown in Figure 7b. Accompanying each increment of material yielding is an accommodation to the load. Ultimately, the cells are collapsed, the area that the material presents to the load is increased through barreling, and the applied load rises precipitously as deformation proceeds.

It was the purpose of this materials development to alter the usual metals behavior pattern, as shown in Figure 7b, toward a load deformation pattern which approaches that represented as the ideal. It was obvious that such parameters as hardness, cell size distribution, ductility, and material quality, exercised some contribution toward the nature of the load deformation pattern. Since very little background exists for predicting the desired type of material behavior, it was necessary to proceed with screening of available materials toward the end of developing a more definitive direction for further material development.

Load Deformation Characteristics

A much broader range of materials was investigated than will be discussed in detail in this report. Many of the materials revealed similar behavior patterns which, it will be shown, can be correlated on the basis of known mechanical properties of the materials. Those specific tests which will be discussed will tend to demonstrate the relationship between mechanical properties and the load deformation pattern of the material in cellular form. Figure 8 shows a portion of the load deformation curve of three commercial aluminum-magnesium alloys of progressively higher alloy content. The cell structure was produced with the standard distribution aggregate. The figure shows that the deformation pattern corresponds with that described for Figure 7b, and the effect of increasing the alloy content is limited to raising the strength level.

The 220-T4 material, with a single sieve fraction cell distribution and with a broadly mixed cell size distribution, was tested. The basic deformation pattern was not altered by these changes. Figure 9 shows the physical changes occurring with these classes of materials as deformation proceeds.

As a result of the screening tests of the various materials systems, cell size distributions, and specimen geometries, an interesting deformation pattern was observed for the composite material which contained the Kanamite ceramic spheres in a matrix of 43 alloy. Figure 10 is a copy of the test record of this specimen. Of all the materials tested up to that time,

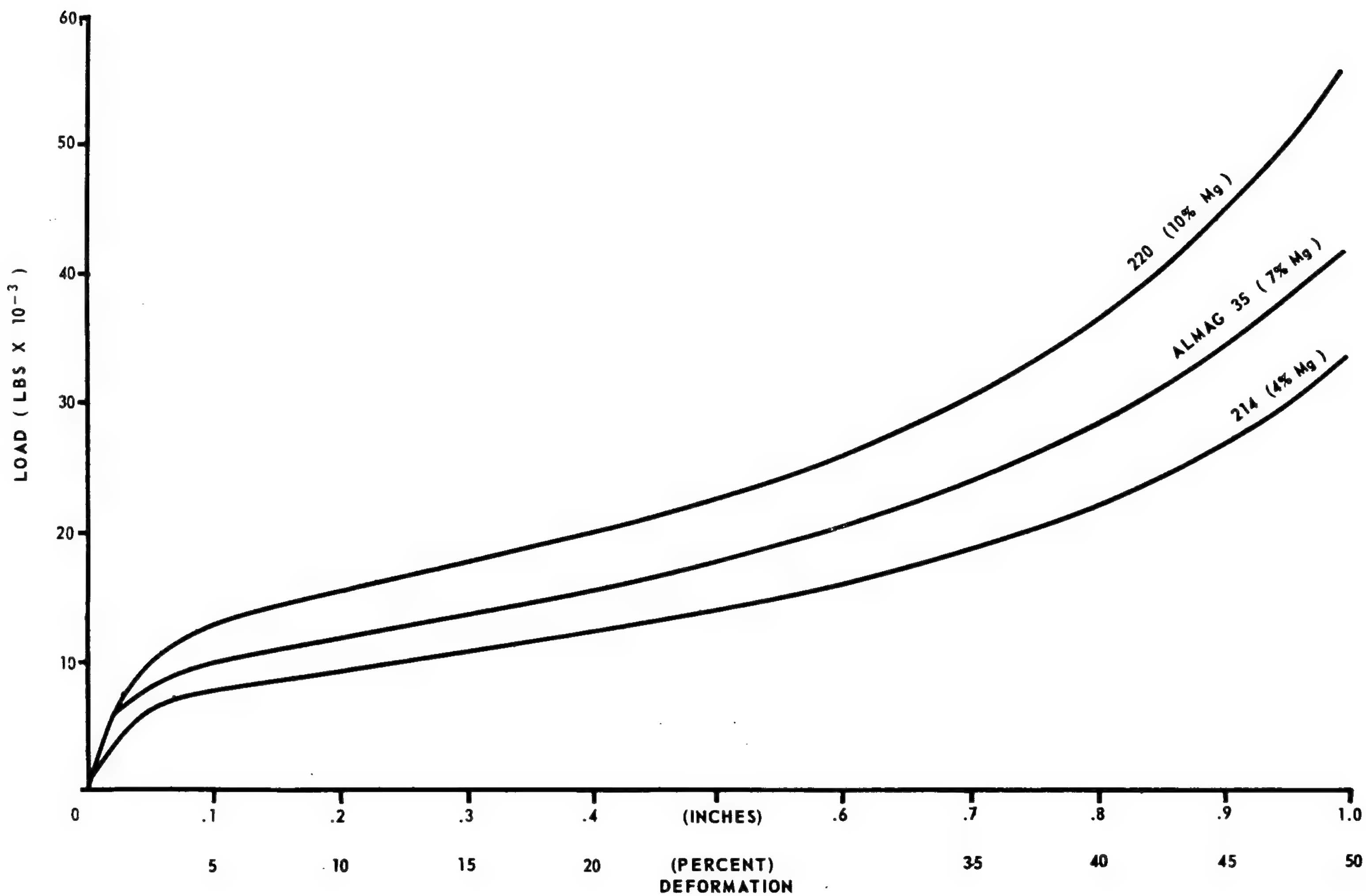

Cell Structure: Standard Distribution; 1/d = 2.00

Figure 8. Compression Test Record of Cellular Aluminum-Magnesium Alloys

C

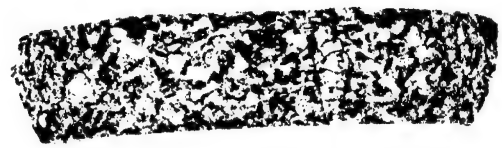

E

B

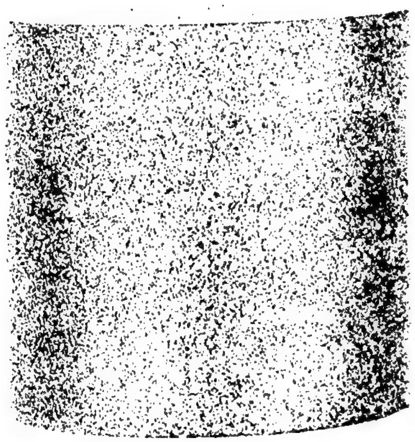

A

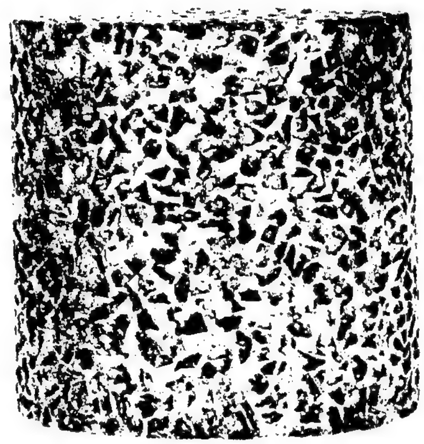

D

Alloy: 214 Test Rate: 0.3 in./min. Mag: 1X

Figure 9. Compression Specimens

Single Structure	Duplex Structure
A - 0% Compression	D - 0% Compression
B - 50% Compression	E - 70% Compression
C - 62% Compression	

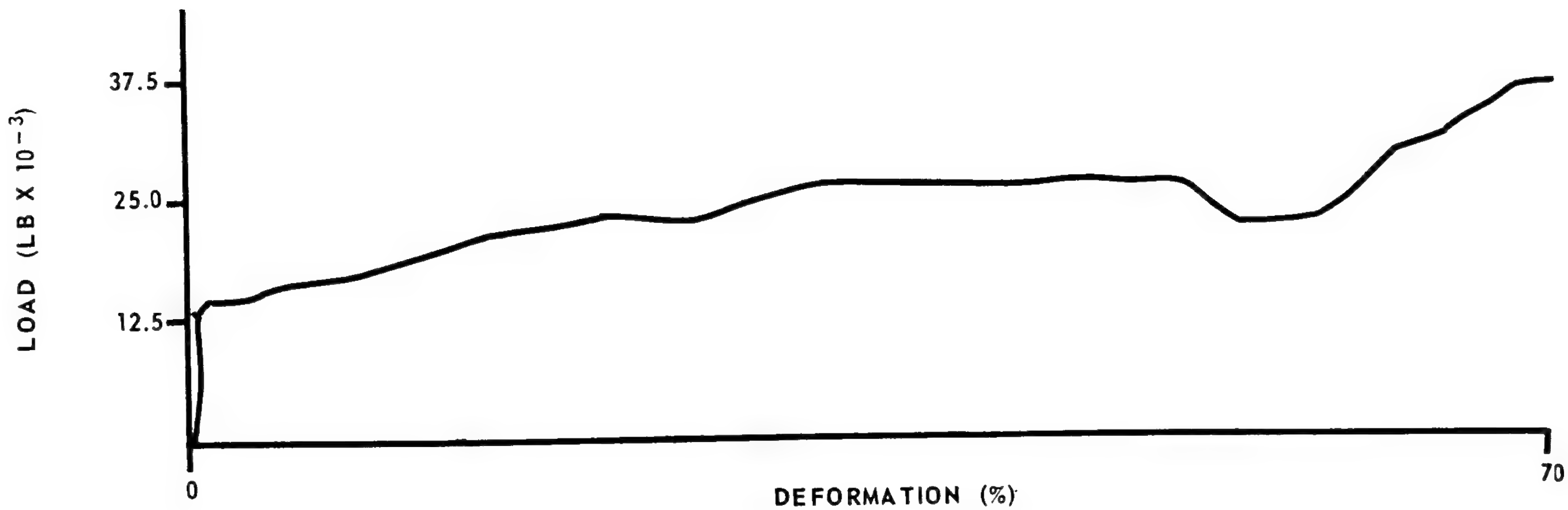

Cell Structure: 20 mesh; l/d = 2.00; Energy Dissipation at 70% = 6200 ft-lb/lb

Figure 10. Load-Deformation Record of 43 Al-Kanamite Composite

this was the only one which seemed to develop a plateau with respect to load. The energy absorption value as calculated from these data was low when compared with some of the other materials. This was due to the higher apparent density of the material. It did, however, provide a clue to the kind of material that was being sought. The test cylinder seemed to crumble under the load in contrast with the more ductile materials which were compressed into flat barreled discs.

At this point the data obtained with the other materials were reviewed. Since none of these load deformation curves could be regarded as approaching the ideal, it was necessary to establish some interim criteria as a basis for selection of materials for further study. In order to do this, the concept of loading ratio was evolved. This was defined as the ratio of load at the point of yielding to the load after a given percentage of deformation. The higher the deformation standard is set, the more significant becomes the loading ratio value. Some of the materials, however, were found to fail catastrophically at deformations of approximately 50 percent.

In order not to exclude these materials from consideration, the loading ratio was defined as the ratio of the load at the point where the material begins to yield to the load at 40 percent deformation. To further aid in this evaluation, the specific energy dissipation realized at 40 percent deformation was calculated. This may be defined as energy dissipation per pound of material. These data are given in Table IV.

The materials with the lowest value for loading ratio and the highest value for specific energy dissipation were regarded as the most promising. It is evident from examination of Table IV that the 7075-T6 material offers the best promise. While some of the materials tested gave lower loading ratio values, the low specific energy dissipation levels reached suggest that their usefulness would be doubtful.

As testing of the 7075-T6 material continued, attention was directed toward preventing catastrophic failure of these specimens, which had been occurring at about 50 percent deformation. Figure 11a shows a specimen ($l/d = 2.56$) at the point where catastrophic failure begins. It will be observed that the mechanism is that of shear. In addition, the failure appears to be analogous to that experienced in the buckling of beams. This suggests that the l/d ratio of the cylinder might have an important bearing on its capacity to support a load beyond 50 percent deformation. If the shear plane which develops terminates at some point where it intersects

TABLE IV. Properties of Energy Dissipation Materials at 40 Percent Deformation

Material		Specific Enery at 40% Deformation (ft-lb/lb)	Loading Ratio[a]
Alloy	Cell Structure		
7075-T6	Std distr	7,600	2.06
7075-T6	Mixed[b]	3,000	1.66
2024-T6	Std distr	6,800	2.15
195-T62	Std distr	5,800	2.85
195-T62	Mixed[b]	1,750	4.00
220-T4	Std distr	5,600	4.00
220-T4	Mixed[b]	3,500	4.00
122-T6	Mixed[b]	3,000	2.00
43[c]	20 mesh	3,000	1.66
Al[c]	20 mesh	2,850	2.30

[a]Load (40% Def)/Load (Initial Yielding)

[b]Equal parts by weight of 6, 8, 10, 20, 30 and 48 mesh

[c]Kanamite filled

a

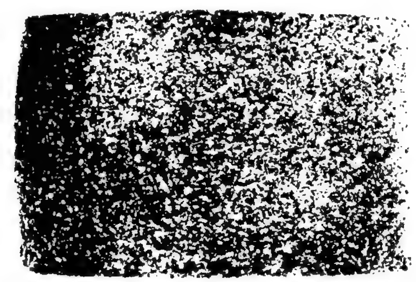

b

a: $l/d = 2.56$
Deformation = 20%

b: $l/d = 1.00$
Deformation = 20%

Figure 11. Effect of l/d ratio on the Deformation of Cellular 7075-T-6 Material

Def = 20%

the plane of the support platen, catastrophic impairment of its ability to support a load would be avoided. Accordingly, a number of specimens with l/d ratios of approximately one were tested. Figure 11b shows a similar material having and l/d ratio of approximately one. Although shear failure will develop at approximately 50 percent deformation, the specimen's favorable l/d ratio will permit it to continue to support a load up to approximately 70 percent or more deformation. Figure 12 shows the stress deformation curve obtained with a similar sample. The energy absorption calculated at the 70 percent deformation level was 15,000 ft-lb/lb.

Summary of Compression Test Data

The complex criteria for evaluation of the energy dissipation characteristics of these materials makes it difficult to compare materials on the basis of the stress deformation curve. One possible method for comparing the data is to calculate the cumulative energy at a number of levels of deformation during compression testing. The specific energy dissipation values are then plotted as the ordinate vs the percent deformation. This method eliminates the effects of dimensional and weight variability in the specimens, clearly defines the specific energy dissipation levels obtainable with the various material systems, and indicates the relationship between degree of deformation and specific dissipation energy. The extent to which a given material approaches ideal behavior, as shown in Figure 7a, is indicated by the shape of its curve. An ideal material of high energy dissipation capacity would be represented by a straight line of steep slope. Figure 13 presents the data obtained with a number of the materials studied as part of this investigation. The curves offer a convenient comparison of data obtained with the various materials. The end point of each curve represents either termination of the test or catastrophic failure of the specimens. The shorter curves represent the latter. All of the materials were tested with specimens having an l/d ratio of approximately two. The exception is the curve which represents the 7075-T6 material having an l/d ratio of 1.28. The only materials which have a linear relationship between deformation and specific energy are the 7075-T6* and the 43 (Kanamite). The higher specific energy capacity of the 7075-T6* material clearly favors the selection of this material.

*l/d = 1.28.

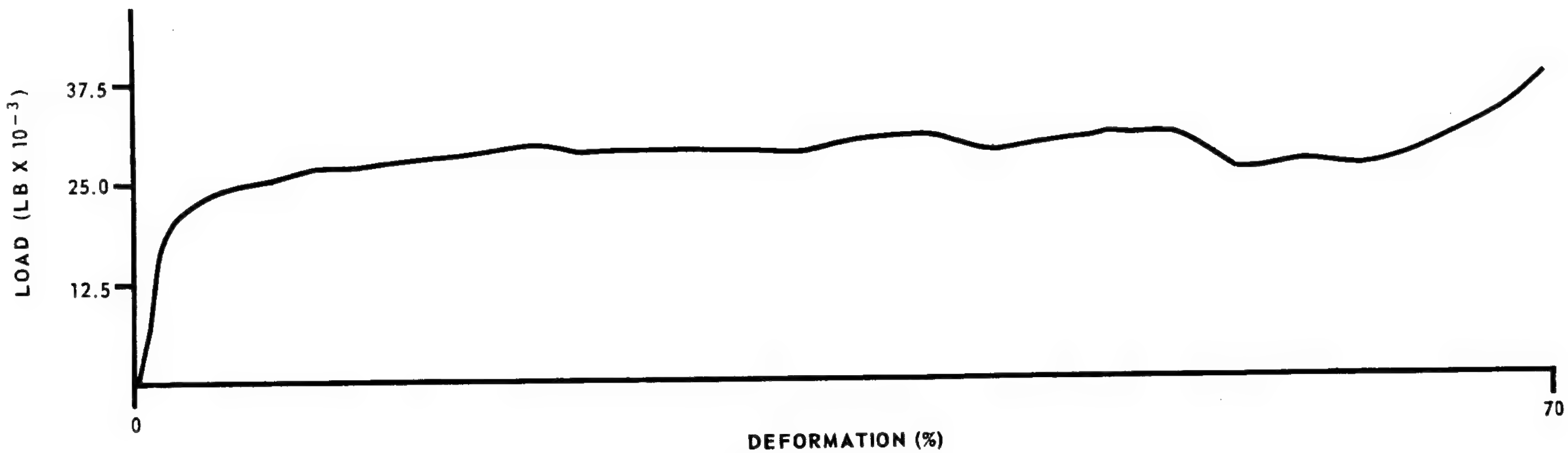

1/d = 1.28 Cell structure: 35 mesh Energy dissipation at 70% = 15,300 ft-lb/lb

Figure 12. Load-Deformation record of 7075-T6 Material

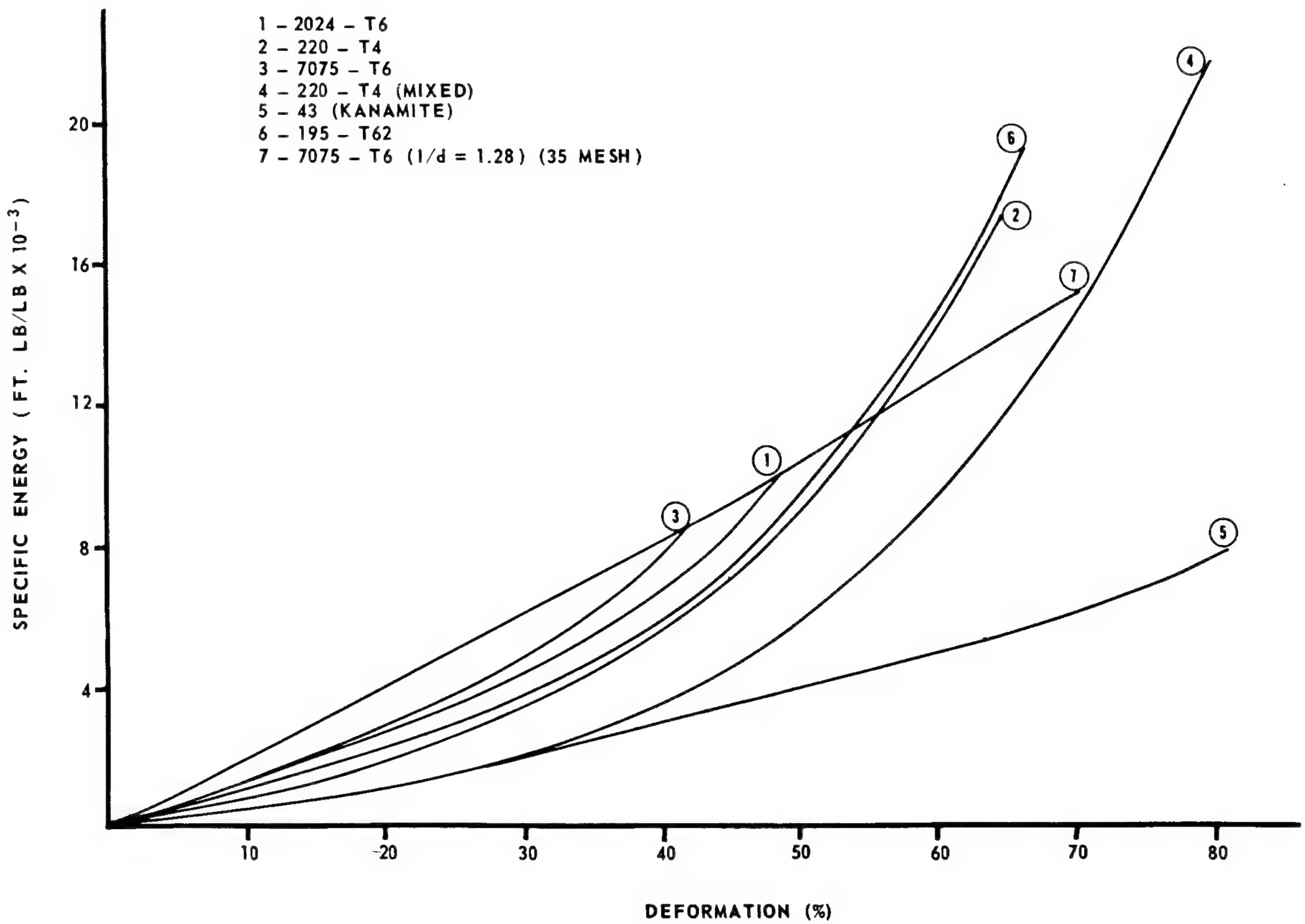

Cell structure: Standard Distribution (unless otherwise noted)
1/d = 2.00

Figure 13. Specific Energy characteristics of Cellular Aluminum Materials

Effect of 1/d Ratio on Deformation Characteristics

A series of samples having 1/d ratios between 0.985 and 2.560 were compression tested. The promising 7075 composition was employed and the cell structure corresponded to the standard distribution aggregate. The load deformation curves have been plotted in Figure 14. Since the deformation is plotted as total rather than unit values, the actual percentage deformation at the significant points on the curve are indicated. The initial dip in the curves marks the onset of shear failure. With 1/d ratios up to approximately two, this onset develops at around 50 percent deformation. The columnar instability of the sample having an 1/d ratio of 2.560 is clearly evident by the sharply lower deformation percentage at which shear failure begins (18 percent). Further examination of these curves shows that at 1/d ratios below 1.5 the load bearing ability of the sample is not severely impaired by the onset of shear failure. However, as this ratio becomes larger, the shear failure leads to catastrophic collapse of the test cylinder. Reference may again be made to Figure 11 which shows the mode of failure for cylinders of high and low 1/d ratios. The unit compressive properties of these test cylinders have been calculated and are shown in Table V.

Effect of Two-Sieve Fraction Cell Structure on Deformation Characteristics

Two groups of specimens were prepared in order to evaluate the deformation pattern resulting from a cell structure composed of two widely separated, but narrow, ranges of cell size distributions. The common cell size for both groups corresponded to a 35 mesh sieve fraction of aggregate making up 50 percent of the volume of the material. One group had as its remaining 50 percent a larger 20 mesh fraction; the other group had a smaller 48 mesh fraction as its remaining 50 percent. The 1/d ratio of these specimens was set at approximately 1.2.

The compression test curves obtained with these samples are shown in Figure 15. For comparative purposes, the curve obtained with the standard distribution sample (1/d = 1.470) is plotted on the same graph at the same scale. Since all of these samples were prepared and heat treated at the same time, the data should be directly comparable. The unit compressive properties of these materials are also included in Table V.

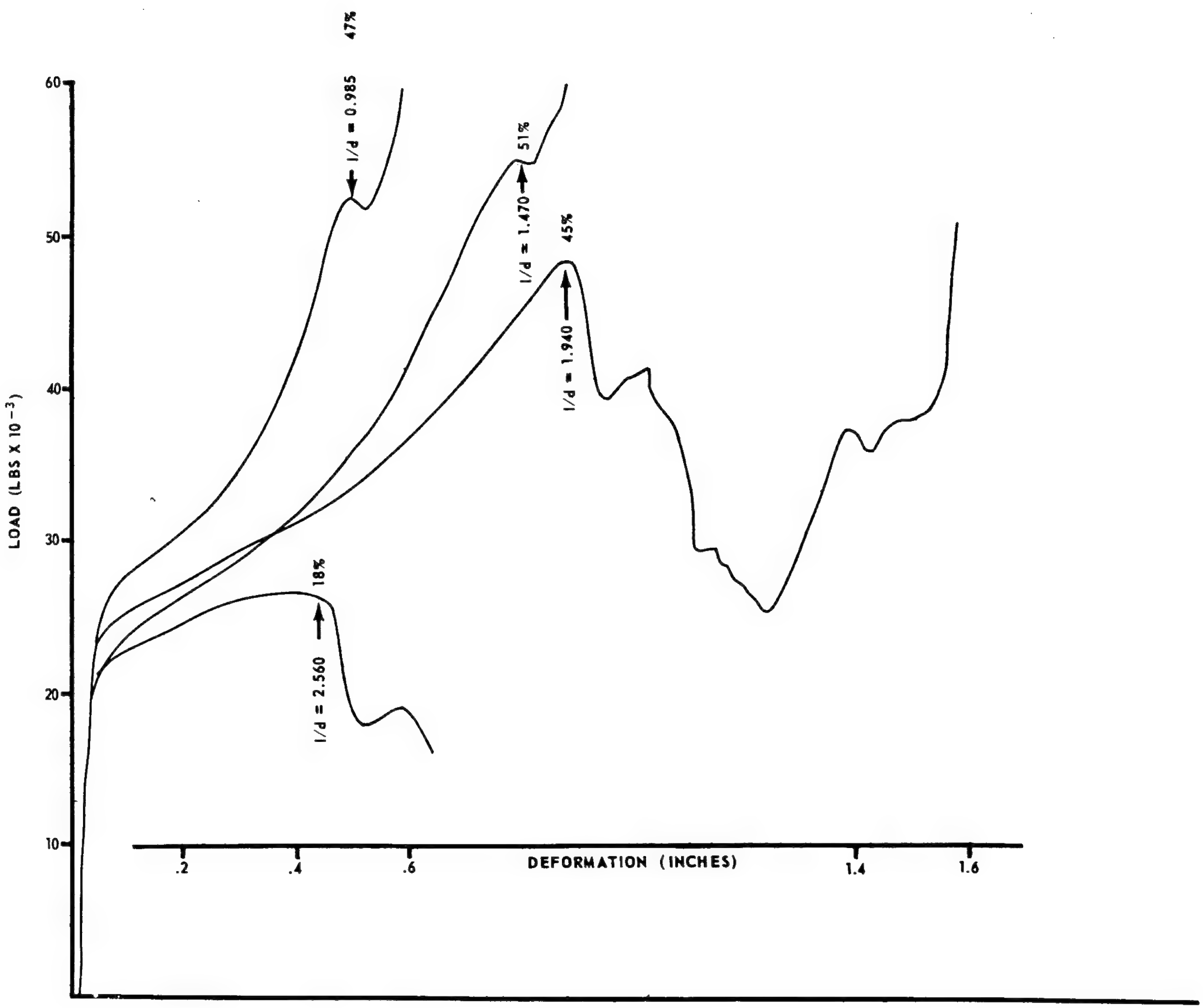

Figure 14. Effect of l/d ratio on Compressive Properties

TABLE V. Compressive Properties of 7075-T6 Cellular Test Cylinders

Cell Size	l/d Ratio	Compressive Properties: Strength (psi) Yield	Compressive Properties: Strength (psi) Ultimate[a]	Compressive Properties: Deformation (%)	Loading Ratio*	Apparent Density (g/cc)
Standard distribution	0.985	7,700	15,500	47	2.00	1.07
Ditto	1.470	6,500	16,400	51	2.52	1.00
Ditto	1.940	7,300	14,000	45	1.92	1.01
Ditto	2.560	6,700	8,300	18	1.24	1.09
50%: 35 Mesh	1.200	4,300	12,300	51	2.86	0.95
50%: 20 Mesh	1.140	4,400	10,000	55	2.27	0.95
50%: 35 Mesh	1.185	4,500	12,800	51	2.84	0.93
50%: 48 Mesh	1.205	3,500	11,200	52	3.20	0.90
100%: 35 Mesh	1.280	7,300	9,000	52	1.25	0.94

[a] Strength deformation and loading ratio at start of shear failure.

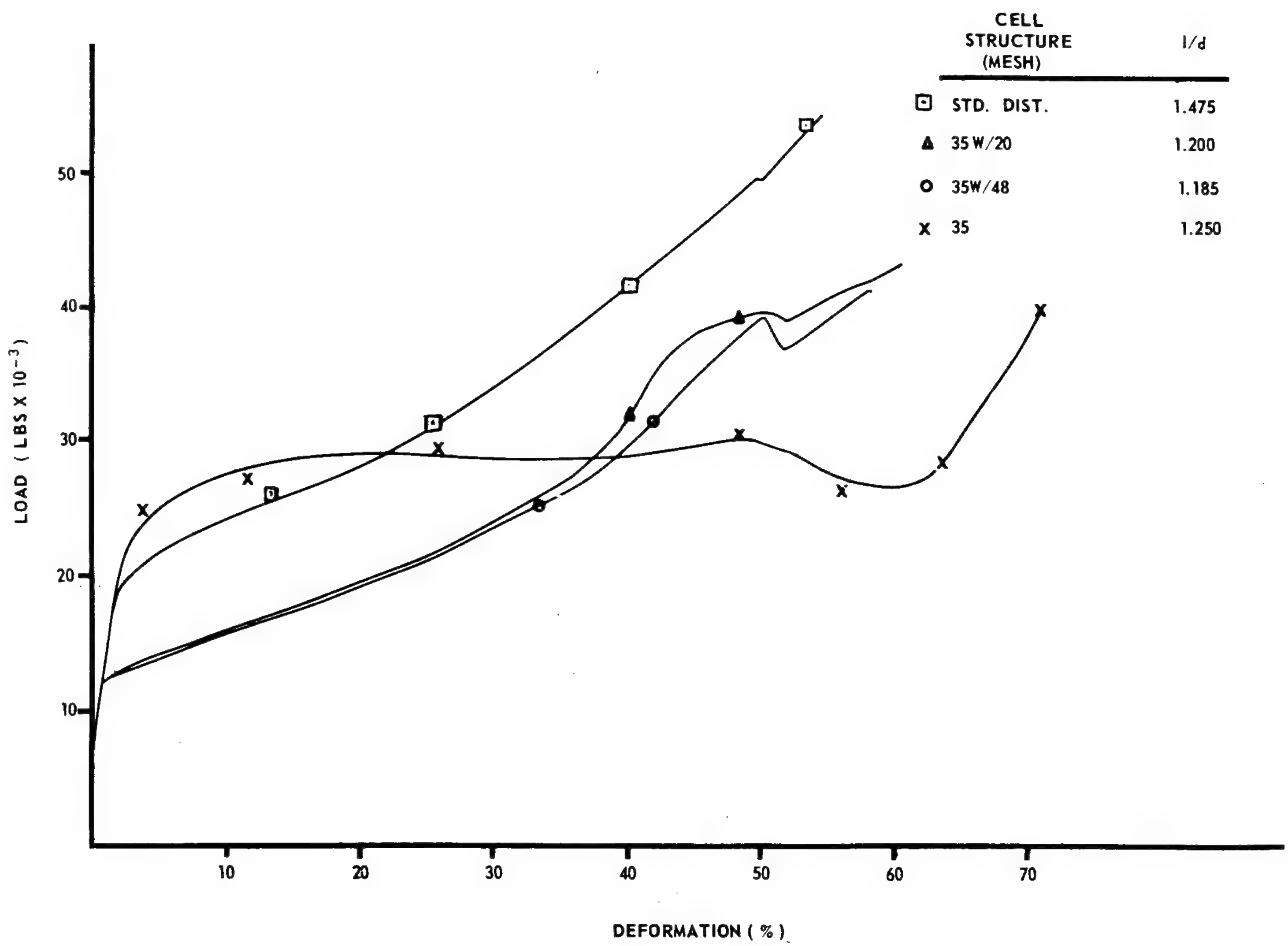

Figure 15. Effect of Cell Structure on Compressive Properties of 7075-T-6 Aluminum Alloy

Examination of these data indicates that one of the effects of the two-sieve type structure is to lower the compressive yield strength of the material. One possible explanation for this effect may be that in a structure which contains two widely separated cell size fractions, the larger cells are inherently less strong than the smaller cells. This may be illustrated schematically, as shown in Figure 16.

This figure shows a representation of a two-sieve fraction structure (Figure 16a). It will be noted that the cell walls are themselves a porous or cellular structure. The inset (Figure 16b) shows that the cell walls which surround the small cell fraction are solid metal. When such a material is loaded in compression, it would be expected that the first cells to collapse would be the larger ones and that this would occur at a lower load than would be the case if no small cells were present in the structure. As the load increases, the specimen accommodates to the load until the smaller cells become the principal means for support. Further deformation then proceeds at higher loads because of the greater inherent strength of the smaller cells. The whole structure, however, is inherently inferior to a uniform cell size material, hence the lower strength of the two-cell material. A corollary of this analysis is that the optimum strengths would be obtained with a uniform cell size material. In addition, a uniform cell size structure should tend to lower the value for loading ratio, since deformation would start at a higher load level. This hypothesis was verified by testing such a material, and these data are included in Figure 15. Sample cylinders from this lot were selected for submission to NASA Langley Field, for evaluation of the material at its current state of development.

Heat Treatment of 7075 Alloy

Since the 7075 composition is one that has been developed for use as a wrought material, homogenization of the alloy is normally achieved through rolling or extrusion of cast billets. In order to use the material in the cast form, rather drastic heat treatments are necessary to achieve the homogenization ordinarily resulting from working operations. At the present stage of material development this problem remains as an area of uncertainty.

The initial practice adopted was to solution treat the material by means of a two-stage process. The first step was to treat the billets at 860° F for 64 hours and then raise the temperature to 880° F for 24 additional hours before quenching. The material was then aged for 24 hours

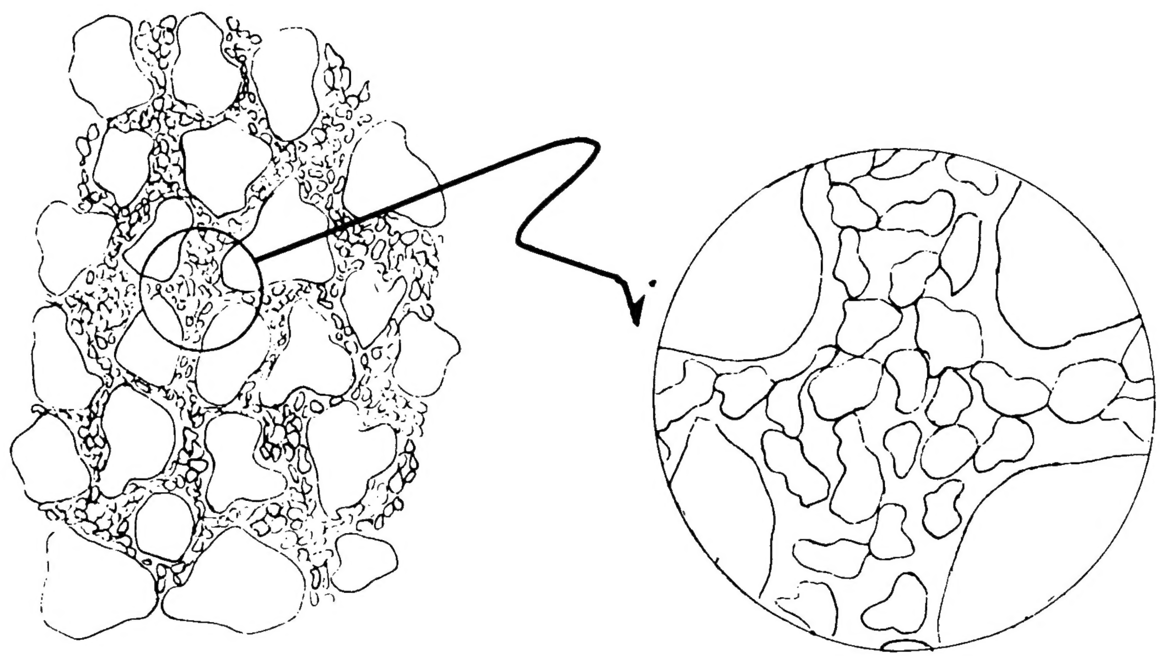

a b

Figure 16. Schematic illustration of Two-sieve Fraction Cell Structure

at 250° F. One of the billets was aged for 48 hours to provide some indication of the aging trend. The hardness levels after treatment were measured and are given below.

Distance from Center of Billet (in.)	Hardness			
	24 hr Age		48 hr Age	
	Dph[a]	Bhn[b]	Dph[a]	Bhn[b]
0	201	170	178	153
0.2	181	156	175	151
0.5	178	153	185	159
0.7	171	148	185	159

[a]1-Kg load

[b]By conversion

Since the nominal Brinell hardness for 7075-T6 is 150, the indications are that the heat treatment was effective. However, additional work will be necessary to establish a correlation between hardness, heat treatment, and the compressive properties of the cellular structure.

REVIEW AND CONCLUSIONS

At the beginning of this study it was assumed that the porous metal material would ultimately be prepared in bulk form and, as a consequence, it would be necessary to establish the degree to which the properties of the material were uniform through its bulk. As the study progressed it became evident that the question of bulk uniformity was of secondary importance compared to developing a material which had satisfactory deformation characteristics. As a result, study of the uniformity of the material was deferred.

On the basis that the objectives of this investigation were to develop cellular metal structures having high load-carrying capacity, low loading ratio values, and maximum compressiblity, the following conclusions are drawn:

1. Cellular cylinders of 7075-T6 material having uniform cell size and appropriate l/d ratios can provide for at least 15, 000 ft-lb/lb of energy dissipation when the cylinder height has been reduced by 70 percent.

2. High strength compositions heat treated to optimum strength levels offer the best promise for dissipation of energy at relatively constant levels of loading.

3. Uniform cell size in the cellular structure favors uniform loading through the compressive deformation of the material.

4. High l/d ratios (more than 1.5) result in columnar instability and early catastrophic failure of the material.

NASA-Langley, 1964 CR-93

"The aeronautical and space activities of the United States shall be conducted so as to contribute . . . to the expansion of human knowledge of phenomena in the atmosphere and space. The Administration shall provide for the widest practicable and appropriate dissemination of information concerning its activities and the results thereof."

—National Aeronautics and Space Act of 1958

NASA SCIENTIFIC AND TECHNICAL PUBLICATIONS

TECHNICAL REPORTS: Scientific and technical information considered important, complete, and a lasting contribution to existing knowledge.

TECHNICAL NOTES: Information less broad in scope but nevertheless of importance as a contribution to existing knowledge.

TECHNICAL MEMORANDUMS: Information receiving limited distribution because of preliminary data, security classification, or other reasons.

CONTRACTOR REPORTS: Technical information generated in connection with a NASA contract or grant and released under NASA auspices.

TECHNICAL TRANSLATIONS: Information published in a foreign language considered to merit NASA distribution in English.

TECHNICAL REPRINTS: Information derived from NASA activities and initially published in the form of journal articles.

SPECIAL PUBLICATIONS: Information derived from or of value to NASA activities but not necessarily reporting the results of individual NASA-programmed scientific efforts. Publications include conference proceedings, monographs, data compilations, handbooks, sourcebooks, and special bibliographies.

Details on the availability of these publications may be obtained from:

SCIENTIFIC AND TECHNICAL INFORMATION DIVISION

NATIONAL AERONAUTICS AND SPACE ADMINISTRATION

Washington, D.C. 20546